Biophysical Journal, Volume *120*

Supplemental information

Depletion of HP1α alters the mechanical properties of MCF7 nuclei

Susav Pradhan, Raoul Solomon, Ankita Gangotra, Gleb E. Yakubov, Geoff R. Willmott, Catherine P. Whitby, Tracy K. Hale, and Martin A.K. Williams

Manuscript submitted to **Biophysical***Journal*
Article

Depletion of HP1α alters the mechanical properties of MCF7 nuclei

Susav Pradhan[1,2], Raoul Solomon[1], Ankita Gangotra[2,3], Gleb E. Yakubov[4,5], Geoff R. Willmott[2,3,4], Catherine P. Whitby[1,2], Tracy K. Hale*[1], and Martin A.K. Williams*[1,2]

[1]School of Fundamental Sciences, Massey University, Palmerston North 4442, New Zealand.
[2]The MacDiarmid Institute for Advanced Materials and Nanotechnology, Wellington, New Zealand.
[3]Department of Physics, The University of Auckland, New Zealand.
[4]School of Chemical Sciences, The University of Auckland, New Zealand.
[5]School of Chemical Engineering, The University of Queensland, Brisbane, Australia.
[6]School of Biosciences, Faculty of Science, University of Nottingham, Nottingham, United Kingdom.
*Correspondence: T.K.Hale@massey.ac.nz; M.Williams@massey.ac.nz.

SUPPLEMENTARY MATERIAL

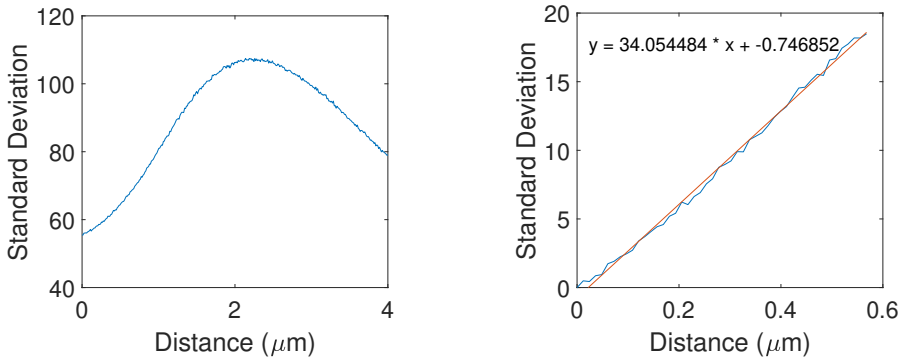

(a) (b)

Figure S1: Conversion of the standard deviation of the average intensity values of images of beads as the height of the bead changes relative to the focus of microscope. (a) Change of Intensity values as a function of bead moved. (b) Fitting the linear region of Fig. (a) to extract the slope, which gives the conversion factor.

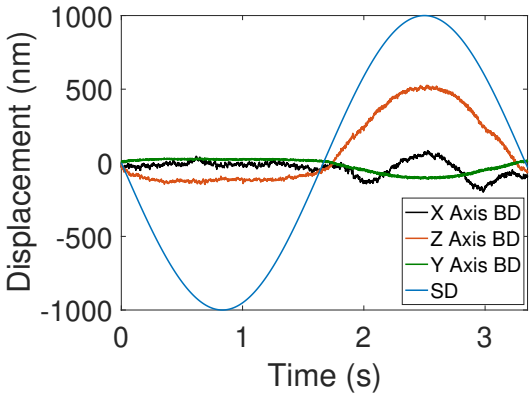

Figure S2: Displacement of the stage and of the bead in the trap during the experiment. The sinusoidal movement of the stage produces bead displacements in X, Y and Z. In the first half of the period, the cell moves down and hence the bead diffuses freely in the trap. At the beginning of the second half of the period, when the cell intercepts the bead and pushes it up, the displacement of the bead in Z begins to be significant and it is accompanied by smaller lateral displacements in X and Y.

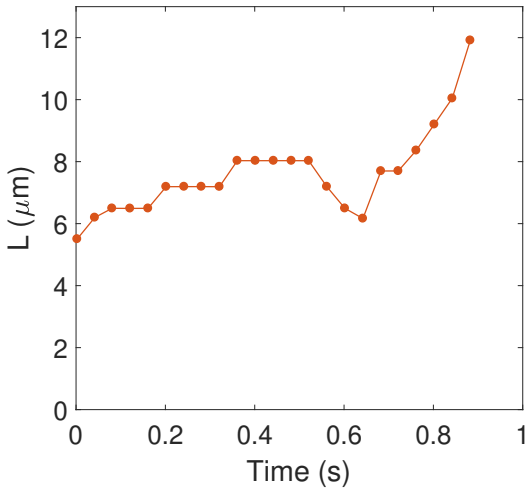

Figure S3: An example of aspiration data obtained using optical microscopy. The aspirated length (L) is plotted as a function of time for an MCF7 (control) nucleus passing into a pipette of inner diameter 5.5 μm with applied suction pressure of 50 mbar. The time resolution (24 Hz) is lower than for the electronic signals (300 Hz).

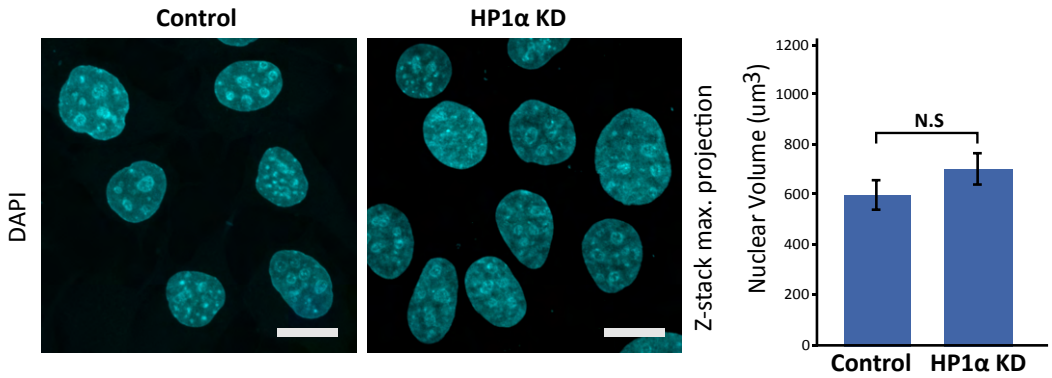

(a)

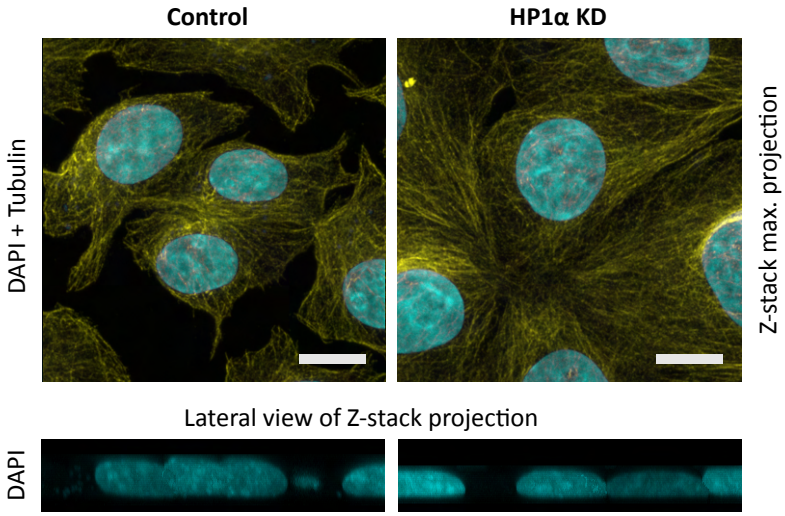

(b)

Figure S4: (a) Representative confocal microscopy images of z-stack maximum intensity projections from MCF7 control and MCF7 HP1α KD cells stained with DAPI to detect DNA (*cyan*), with a graph showing the average volume of the nuclei n=28, ± standard error, not significant (n.s) at $p < 0.01$ (*t* - test). Scale bars - 20 μm. (b) Representative confocal microscopy images of z-stack maximum intensity projections from MCF7 control and MCF7 HP1α KD cells growing asynchronously in 2-D culture stained with DAPI to detect DNA (*cyan*) and an antibody directed against α-Tubulin to show the cytoskeleton (*yellow*). Scale bars - 20 μm. The bottom panel is a 90° rotation of the above z-stack maximum intensity projection showing the DNA (*cyan*).

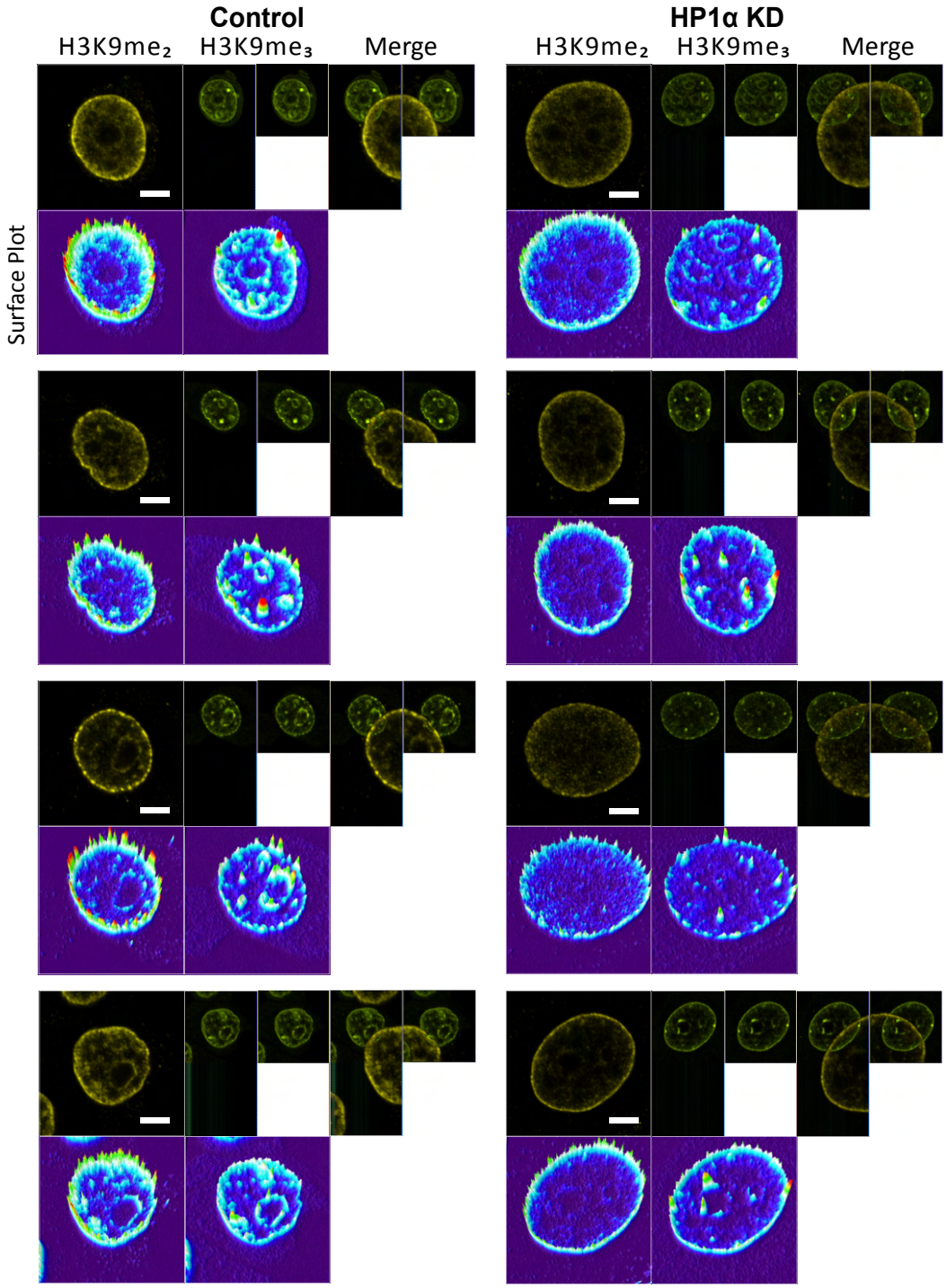

Figure S5: Immunofluorescence confocal microscopy images of MCF7 control and MCF7 HP1α KD cells stained with antibodies against H3K9me2 (*yellow*) and H3K9me3 (*magenta*). Fluorescense surface plots of the medial slices through the nuclei demonstrate the intensity of antibody staining. Scale bars - 5 μm.

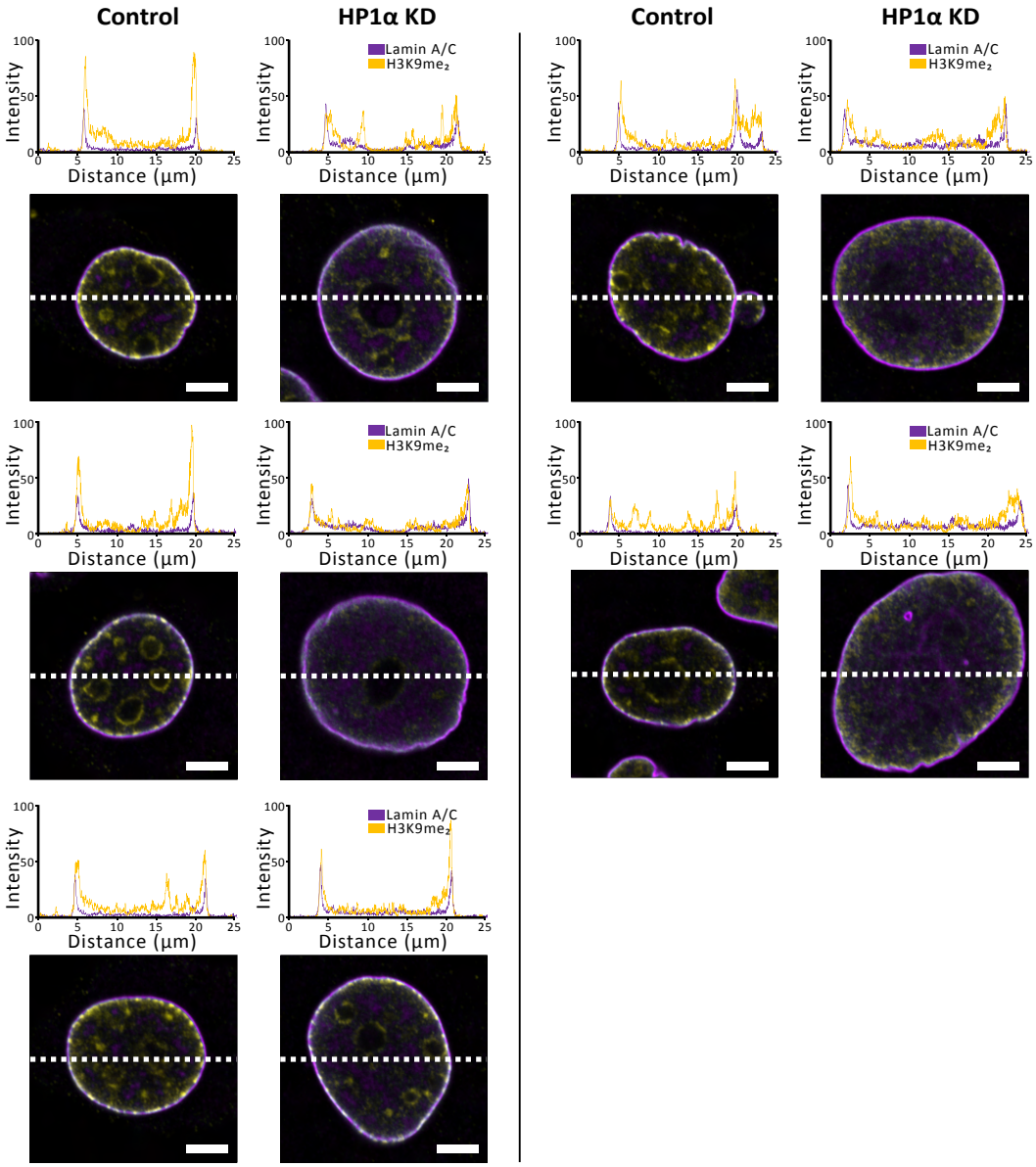

Figure S6: Confocal microscopy medial sections of individual nuclei from MCF7 control and MCF7 HP1α KD cells stained with antibodies against Lamin A/C (*magenta*) and H3K9me2 (*yellow*). Above each medial slice are line plot profiles of fluorescence intensity (percentage of grey value saturation). Scale bars - 5 μm.

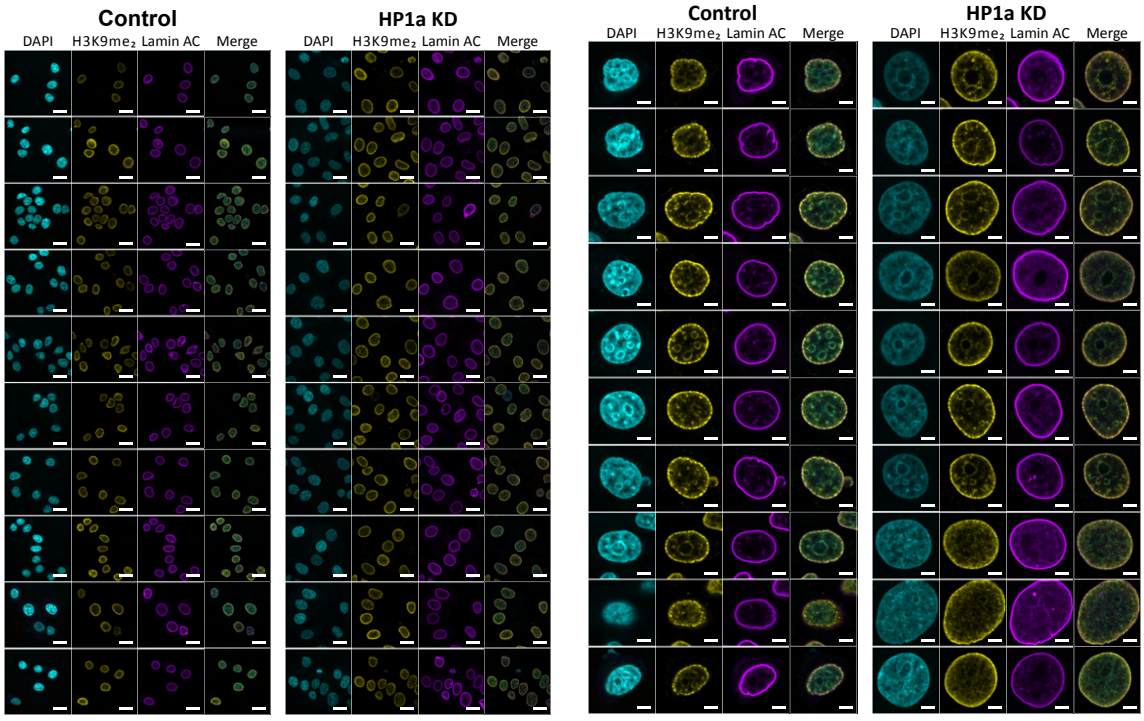

(a) (b)

Figure S7: Confocal microscopy medial sections of MCF7 control and MCF7 HP1α KD cells stained with DAPI to detect DNA (*cyan*) and antibodies against H3K9me2 (*yellow*) and Lamin A/C (*magenta*). (a) Scale bars - 20 μm. (b) Scale bars - 5 μm.

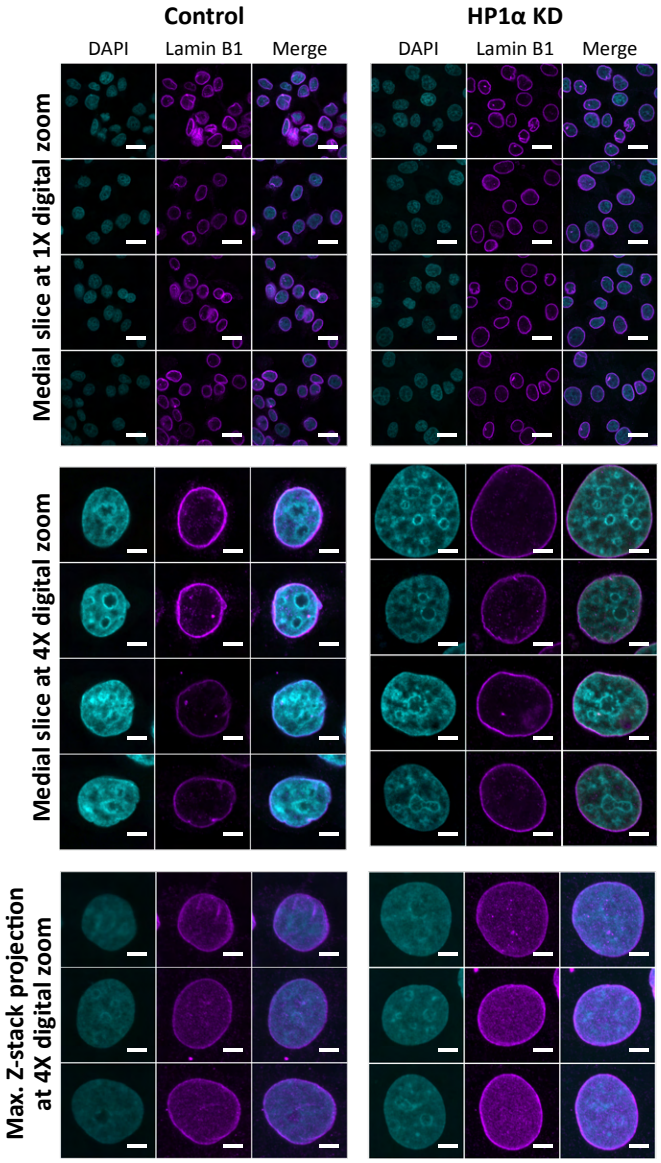

Figure S8: Confocal microscopy images from MCF7 control and MCF7 HP1α KD cells stained with DAPI to detect DNA (*cyan*) and an antibody against Lamin B1 (*magenta*). Top panel, medial slices, scale bars - 20 μm. Middle panel, medial slices at 4x zoom, scale bar - 5 μm. Bottom panel, maximum projection of Z-stacks at 4x zoom, scale bar - 5 μm.

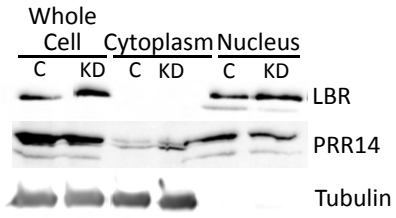

Figure S9: Whole and fractionated cell lysates from an equal number of MCF7 control or HP1α KD cells were analysed by immunoblotting with an antibody against Lamin B receptor (LBR), PRR14, and α-Tubulin as a control for the cytoplasmic fraction.

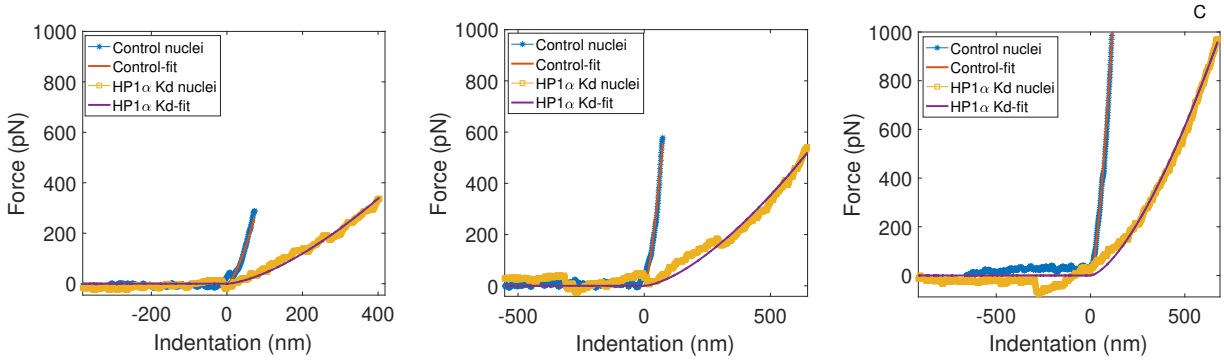

(a) (b) (c)

Figure S10: Hertzian curve fitting on three different sweeps from zero to maximum force of (a) 300 pN, (b) 500 pN and (c) 1 nN for Control and HP1αKD nuclei.

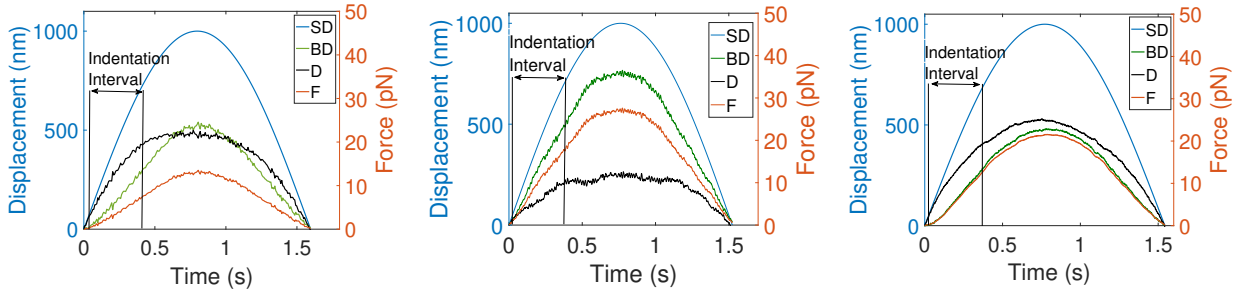

(a) (b) (c)

Figure S11: Temporal sequences of indentation intervals for (a) longitudinal (HP1αKD), (b)lateral indentation (Control) and (c) lateral indentation (HP1αKD).

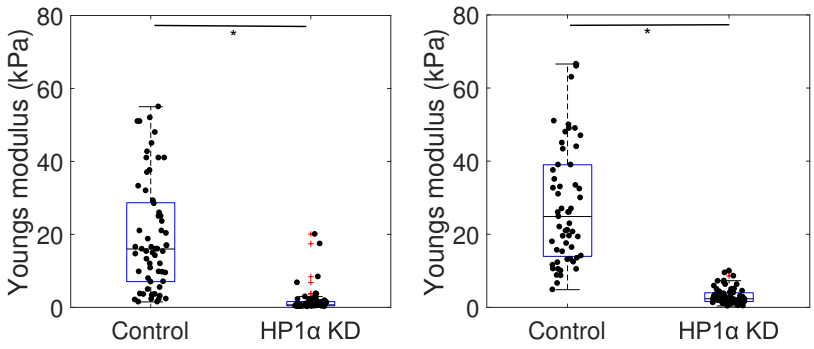

(a) (b)

Figure S12: Apparent Young's modulus obtained using AFM data for maximum force of (a) 0.3 nN and (b) 1 nN (*$p < 0.0001$).

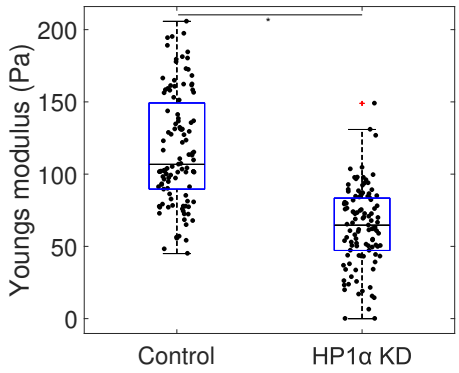

Figure S13: Comparison of Apparent Young's modulus for control and HP1α KD whole MCF7 cells (*p < 0.0001).

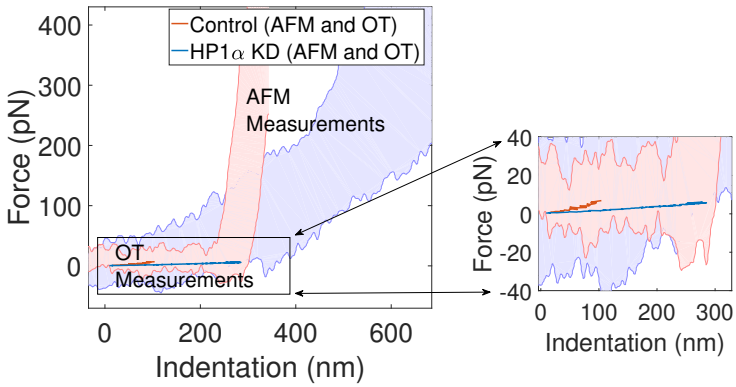

Figure S14: Comparison of force indentation plots for control and HP1α KD nuclei using AFM and OT. The AFM data has been arbitrary shifted to show that OT detects contact earlier than AFM.

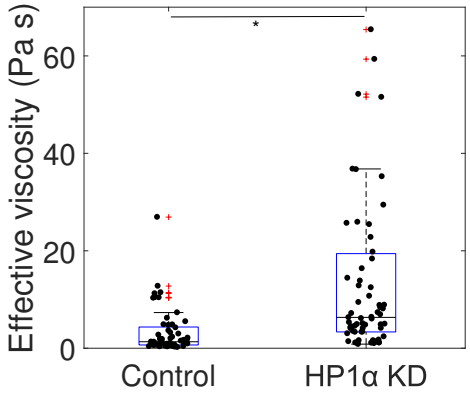

Figure S15: Comparison of Effective viscosity for the viscoelastic model for control and HP1α KD whole MCF7 cells (*p < 0.05).